

# Electronic structure of the 1,3,5-tridehydrobenzene triradical in its ground and excited states

Lyudmila V. Slipchenko and Anna I. Krylov

Department of Chemistry, University of Southern California, Los Angeles, California 90089-0482

(Received 8 January 2003; accepted 5 March 2003)

The ground and low-lying electronic states of the 1,3,5-tridehydrobenzene triradical are characterized by electronic structure calculations. It is found that the ground state is the  ${}^2A_1$  doublet of  $C_{2v}$  symmetry. Another doublet state lies 0.1–0.2 eV higher in energy, and the lowest quartet state of  $D_{3h}$  symmetry is 1.2–1.4 eV higher in energy. Both doublets are degenerate at  $D_{3h}$  geometries and undergo different Jahn–Teller distortions. Structurally, the triradical is tighter than the parent neutral molecule (benzene), because the interaction among the unpaired electrons results in additional bonding even in the high-spin state (quartet). The adiabatic doublet–quartet energy gap and the excitation energies calculated at the equilibrium geometries of the 3,5-dehydrophenyl anion are provided to aid in the design and interpretation of photoelectron experiments. © 2003 American Institute of Physics. [DOI: 10.1063/1.1569845]

## I. INTRODUCTION

Triradicals are molecules with three unpaired electrons. From the electronic structure point of view, they are species where three electrons are distributed in three (near) degenerate orbitals. This definition is an extension of Salem and Rowland's definition of diradicals as molecules with two electrons occupying two (near) degenerate orbitals.<sup>1</sup> Because of the more extensive electronic degeneracy, the *ab initio* modeling of triradicals is even more complicated than that of diradicals. Contrary to diradicals, which often appear as intermediates or transition states in chemical reactions, triradicals are less common and their studies are scarce.<sup>2–5</sup> The interest in triradicals and other species with several unpaired electrons stems from their role as building units of organic magnets.<sup>6–11</sup>

A number of radical and diradical benzene's derivatives (i.e., phenyls and benzyne) have been extensively studied both experimentally and theoretically.<sup>12–19</sup> However, the corresponding triradical analog, 1,3,5-tridehydrobenzene ( $C_6H_3$ ), has not attracted considerable attention yet. Bettinger *et al.*<sup>20</sup> have reported the equilibrium structure of the  ${}^2A_1$  ground state of this molecule calculated by the coupled cluster with single and double excitations (CCSD) method in a polarized double- $\zeta$  basis. Recently, Lardin *et al.* determined the heat of formation and bond dissociation energies of 1,3,5-tridehydrobenzene.<sup>21</sup> Positive and negative ions of 1,3,5-tridehydrobenzene have also been studied.<sup>22–25</sup> The most interesting feature of the didehydrophenyl cation is the so called double aromaticity.<sup>22,23</sup> In addition to an aromatic  $\pi$  system, there is a bonding  $\sigma$  system derived from the unpaired electrons. While the cation is a closed-shell system, the corresponding anion is of a diradical type. It was concluded from its reactivity<sup>25</sup> that the ground state of the anion is a singlet (in violation of Hund's rule).

The present study investigates the electronic structure of the ground and lowest electronically excited states of 1,3,5-tridehydrobenzene. We report accurate equilibrium structures

and frequencies, vertical and adiabatic excitation energies, and analyze the bonding. The energy separations between states and their vibrational frequencies can aid in interpreting photoelectron spectra of the 3,5-dehydrophenyl anion. Such spectra should provide the experimental evidence of the electronic structure of 1,3,5-tridehydrobenzene.

The structure of the paper is as follows: the next section discusses methodological issues relevant to triradicals, outlines the spin-flip (SF) approach and describes how it can be extended to triradicals. The results and discussion are presented in Sec. III. Our concluding remarks are given in Sec. IV.

## II. THEORETICAL METHOD AND COMPUTATIONAL DETAILS

### A. Electronic structure of triradicals

In a triradical, three electrons are distributed in three nearly degenerate orbitals. All the relevant Slater determinants with a positive projection of the total spin are shown in Fig. 1. The high-spin determinant (1) has  $M_s=3/2$ . Nine determinants have  $M_s=1/2$ , six of them [(5)–(10)] being of a closed-shell type (these are the eigenfunctions of  $\hat{S}^2$ ) and three [(2)–(4)] of an open-shell type (these are not the eigenfunctions of  $\hat{S}^2$ ). Figure 2 shows valid wave functions which can be constructed from the determinants of Fig. 1. From the open-shell determinants (2)–(4), one can construct one quartet (b) and two doublet states (c), (d). These wave functions are eigenstates of both  $\hat{S}_z$  and  $\hat{S}^2$ . Regardless of the spatial symmetry of the orbitals  $\phi_1$ – $\phi_3$ , the closed-shell determinants can form several doublet wave functions (e)–(j), as shown in Fig. 2. The values of  $\lambda$  depend upon the energy separation between the orbitals; i.e., large  $\lambda$  values correspond to nearly degenerate orbitals. For example, when  $\phi_2$  and  $\phi_3$  are exactly degenerate, two different doublet states (i) and (j) are obtained by taking the sum and the difference of determinants (7) and (8). Similarly to the closed-shell

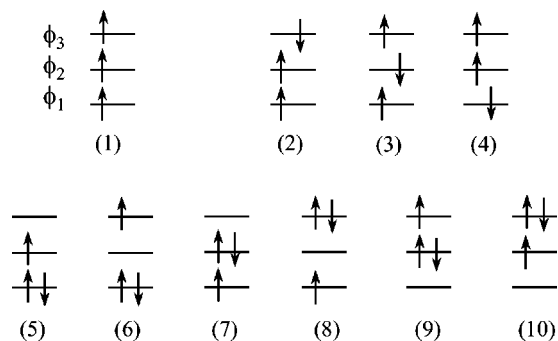


FIG. 1. Slater determinants that can be generated by distributing three electrons over three orbitals. Only determinants with a positive projection of the total spin are shown. Determinant (1) has  $M_s = 3/2$ ; determinants (2)–(10) have  $M_s = 1/2$ . With respect to high-spin determinant (1), all low-spin determinants (2)–(10) are formally singly excited configurations including the spin flip of one electron. By reversing the spins of all the electrons, a set of determinants with  $M_s = -3/2, -1/2$  can be generated. Since spin is not present in the nonrelativistic Hamiltonian, determinants with different  $M_s$  do not interact across the Hamiltonian and, therefore, do not mix in the triradical wave functions. Determinants (1) and (5)–(10) are eigenfunctions of  $\hat{S}^2$ , whereas (2)–(4) are not (however, their proper linear combinations are).

diradicals' singlets, these doublet determinants interact regardless of the orbitals' symmetries. The symmetries of the molecular orbitals (MOs) define which of the configurations shown in Fig. 2 can interact and mix further in the triradical wave functions.

From a methodological perspective, it is important that all the doublets and the low-spin quartet state are multideterminantal. Therefore, a multiconfigurational method should be employed when the triradical orbitals are nearly degenerate. However, if the triradical orbitals are well separated in energy, some of the states [for example, (g) and, perhaps, (e)] can be described by a single-reference method.

Unlike the  $M_s = 1/2$  triradical states, the high-spin component ( $M_s = 3/2$ ) of the quartet state is single determinantal. Moreover, all the low-spin determinants are formally single spin-flipping excitations from the high-spin  $M_s = 3/2$  determinant. Therefore, the SF approach<sup>26–29</sup> can be employed to describe triradicals as explained below.

## B. Spin-flip approach

In the SF approach, one describes low-spin states within a single-reference formalism as spin flipping, e.g.,  $\alpha \rightarrow \beta$ , excitations from a high-spin reference state for which both dynamical and nondynamical correlation effects are much smaller than for the corresponding low-spin states.<sup>26–30</sup> In the case of triradicals, we choose the high-spin ( $M_s = 3/2$ ) component of the quartet state as a reference. This state is accurately described by single-reference methods. The target states, the low-spin component of the quartet and the open- and closed-shell doublets [(b) and (c)–(j), respectively], are described as single-electron excitations including the spin-flip of an electron:

$$\Psi_{M_s=1/2}^{d,q} = \hat{R}_{M_s=-1} \Psi_{M_s=3/2}^q, \quad (1)$$

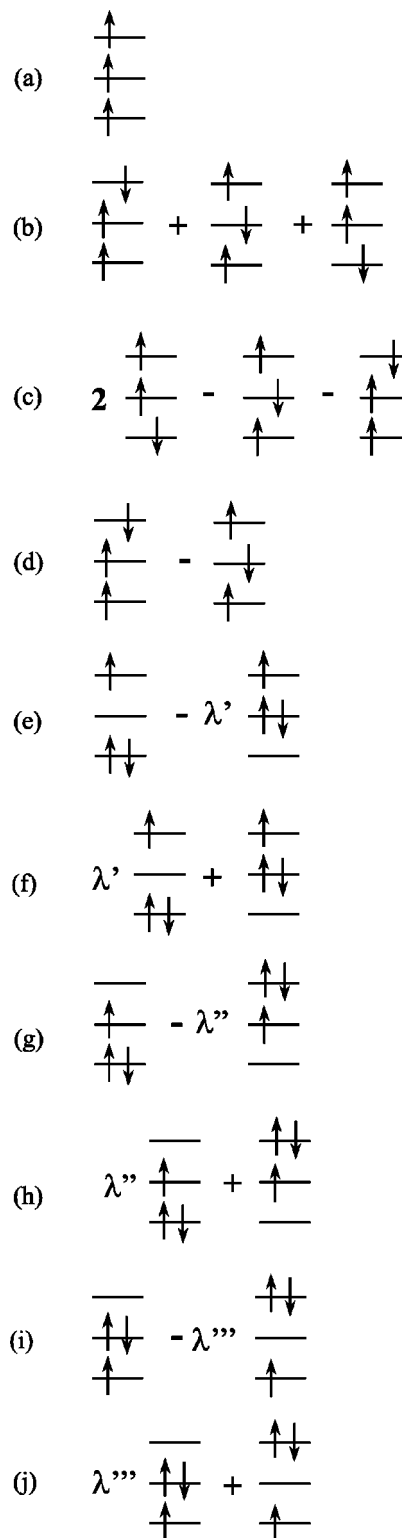


FIG. 2. Triradical wave functions that are eigenstates of  $\hat{S}_z$  and  $\hat{S}^2$ . Symmetry of the orbitals determines if these configurations can interact and further mix with each other. All doublets (c)–(j) and the low-spin component of quartet (b) are multiconfigurational, while the high-spin component of quartet state (a) is singly determinantal.

where  $\Psi_{M_s=3/2}^q$  is the  $\alpha\alpha\alpha$  component of the quartet reference state [(a) from Fig. 2],  $\Psi_{M_s=1/2}^{d,q}$  stands for the final ( $M_s = 1/2$ ) doublet and quartet states [(b)–(j)], and the operator  $\hat{R}_{M_s=-1}$  is an excitation operator that flips the spin of an electron.

By employing theoretical models of increasing complexity for the reference wave function, the description of the final states can be systematically improved. For example, the simplest SF model employs a Hartree–Fock wave function, and the operator  $\hat{R}$  is then truncated at single excitations [SF configuration interaction method with singles (SF–CIS) or SF self-consistent field (SF–SCF)].<sup>26</sup> The spin-complete version of the SF–CIS method was recently developed.<sup>30</sup> The SF–CIS method can be further augmented by perturbative corrections [SF–CIS(D) or SF–MP2].<sup>27</sup> A more accurate description can be achieved by describing the reference wave function by a coupled-cluster model, e.g., CCSD or optimized orbitals coupled-cluster doubles (OO–CCD).<sup>31–33</sup> In this case, the excitation operator  $\hat{R}$  consists of single- and double-excitation operators involving a flip of the spin of an electron (SF–CCSD, SF–OD).<sup>26</sup> Moreover, the SF idea can be used to extend density functional theory to multireference situations.<sup>29</sup> The attractive feature of the SF approach is that it is a multistate (SF–DFT) method; i.e., it describes several states in one calculation. In the case of diradicals, the SF models describe the equilibrium properties of all three diradical states (one open- and two closed-shell singlets) with an accuracy comparable to that of the traditional methods when applied to well-behaved molecules.<sup>27,29,34</sup> We expect the SF methods to describe triradical's states with a similar quality.

### C. Computational details

Equilibrium geometries and vibrational frequencies of the lowest electronically excited states of 1,3,5-tridehydrobenzene have been obtained by using the CCSD model with perturbative triples corrections [CCSD(T)].<sup>35</sup> Adiabatic energy separations have been calculated by the CCSD, CCSD(T), SF–CIS(D), and SF–CCSD approaches. The SF–CCSD method has been used to calculate vertical excitation energies. Additional calculations have been performed by using multiconfigurational self-consistent field (MCSCF) method<sup>36,37</sup> and multiconfigurational quasidegenerate perturbation theory (MCQDPT2).<sup>38</sup> Three basis sets with pure angular momentum polarization functions have been used: the 6-311G\*\* basis,<sup>39</sup> the cc-pVTZ basis,<sup>40</sup> and a mixed basis set [cc-pVTZ on carbon and cc-pVDZ (Ref. 40) on hydrogen]. To calculate the equilibrium geometries of the 1,3,5-tridehydrobenzene anion, the SF–DFT method<sup>29</sup> and the basis set with diffuse functions, 6-311+G\*\*,<sup>39,41</sup> have been used. The basis sets have been obtained from the EMSL database.<sup>42</sup>

To estimate basis set effects, we have also used an extrapolation technique based on an energy separability scheme:

$$E_{SF-CCSD}^{large} = E_{SF-CCSD}^{small} + (E_{SF-CIS(D)}^{large} - E_{SF-CIS(D)}^{small}), \quad (2)$$

where  $E^{large}$  and  $E^{small}$  are the total energies calculated in relatively large (e.g., cc-pVTZ) and small (e.g., 6-311G\*\*) basis sets. This procedure assumes that the changes in the total energy due to the basis set increase are similar for the less and more correlated models [e.g., MP2 and CCSD or SF–CIS(D) and SF–CCSD].

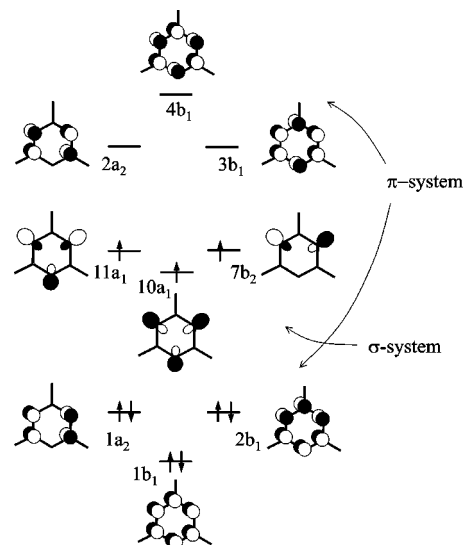


FIG. 3. Molecular orbitals of 1,3,5-tridehydrobenzene at the  $D_{3h}$  symmetry ( $C_{2v}$  labels are used). The  $\pi$  system is as in benzene: orbitals  $1a_2$ ,  $2b_1$  and  $2a_2$ ,  $3b_1$  are degenerate. The  $\sigma$  system consists of three molecular orbitals; two of them ( $11a_1$  and  $7b_2$ ) are exactly degenerate.

All the SF calculations have been performed by using the Q-CHEM (Ref. 43) *ab initio* package. CCSD and CCSD(T) results have been obtained with the ACES II electronic structure program.<sup>44</sup> The multireference calculations have been performed with the GAMESS electronic structure package.<sup>45</sup>

### III. RESULTS AND DISCUSSION

Molecular orbitals of 1,3,5-tridehydrobenzene at  $D_{3h}$  geometry are shown in Fig. 3 ( $C_{2v}$  labels are used). The  $\pi$  system of the molecule is as in benzene: it consists of three doubly occupied bonding orbitals and three virtual antibonding orbitals. Three  $sp^2$ -hybridized orbitals from the carbons that lost their hydrogens form three molecular orbitals of a  $\sigma$  type (these are the  $\phi_1$ ,  $\phi_2$ , and  $\phi_3$  triradical orbitals of Figs. 1 and 2). Two of them,  $11a_1$  and  $7b_2$  ( $\phi_2$  and  $\phi_3$ ), are exactly degenerate at the  $D_{3h}$  geometry (these are the two  $e'$  orbitals). The  $10a_1$  orbital ( $\phi_1$ ) is slightly lower in energy. Energetically, three  $\sigma$  orbitals are located between the bonding and antibonding  $\pi$  orbitals. It is not obvious how three electrons will be distributed in these three  $\sigma$  orbitals. If all three orbitals were exactly degenerate, the ground state of the molecule would be a quartet  ${}^4B_2$  state as dictated by Hund's rule. If, however, the energy gap between the  $10a_1$  and the degenerate  $11a_1/7b_2$  pair were large enough, the ground state would be a doublet state with a doubly occupied  $10a_1$  orbital and a singly occupied  $11a_1$  or  $7b_2$  orbital. In 1,3,5-tridehydrobenzene, one-electron considerations win, and the doublets are lower in energy than the quartet both vertically and adiabatically.

The  ${}^4B_2$  quartet state prefers the  $D_{3h}$  geometry (the appropriate symmetry label is  ${}^4A_2'$ ), with the distances between the radical centers being equal. At its equilibrium geometry, the two doublet states  ${}^2B_2$  and  ${}^2A_1$  are degenerate. By the Jahn–Teller theorem,<sup>46</sup> this degeneracy can be lifted at lower symmetry. The shape of the  $11a_1$  and  $7b_2$  orbitals (see Fig. 3) immediately suggests that the  ${}^2A_1$  doublet will favor a

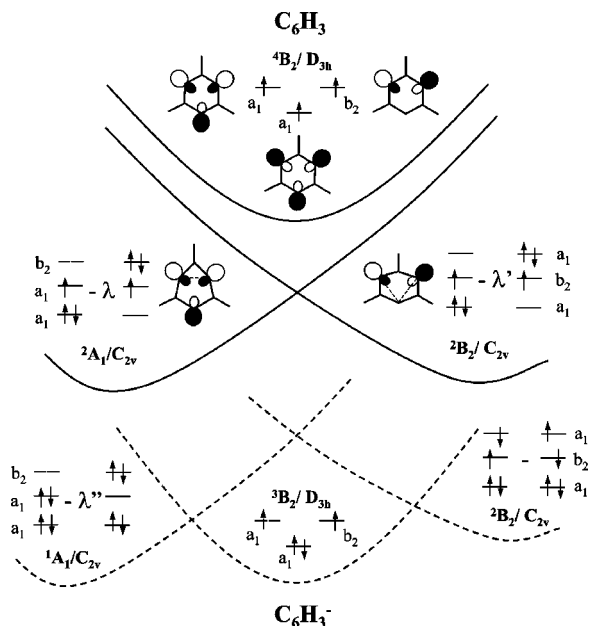


FIG. 4. Jahn–Teller distortions in 1,3,5-tridehydrobenzene ( $C_6H_3$ , upper panel) and in the 1,3,5-tridehydrobenzene anion ( $C_6H_3^-$ , lower panel). The  $^4B_2$  ( $^4A_2'$ ) quartet state of  $C_6H_3$  has  $D_{3h}$  structure for which the  $^2A_1$  and  $^2B_2$  doublets are exactly degenerate. The degeneracy between the doublets can be lifted at lower symmetry. The  $^2A_1$  state is a real minimum, while the  $^2B_2$  doublet is a transition state. The triplet  $^3B_2$  ( $^3A_2'$ ) state of the 1,3,5-tridehydrobenzene anion is of  $D_{3h}$  symmetry. At this geometry, the open and closed-shell singlets are exactly degenerate and can undergo in the Jahn–Teller distortions. The lowest singlet  $^1A_1$  state has  $C_{2v}$  structure.

structure with a shorter distance between the two upper dehydrocarbons. This structure is similar to the structure of m-benzyne in its ground singlet  $^1A_1$  state, in agreement with the recent study of Lardin *et al.*<sup>21</sup> The optimized structure (under  $C_{2v}$  constraint) of the second doublet  $^2B_2$  is less tight and squeezed in a perpendicular direction. This is not a real

minimum but a transition state which connects equivalent minima corresponding to the  $^2A_1$  doublet state.<sup>47</sup> The  $\pi$  system holds the molecule planar and is responsible for the very small amplitudes of the Jahn–Teller distortions.<sup>48</sup> The diagram explaining the energy changes along the two Jahn–Teller distortions is given in Fig. 4.

At  $D_{3h}$  structures, the  $10a_1$  orbital and the degenerate  $11a_1/7b_2$  pair are very close in energy. Subsequently, the wave functions of the both doublets are heavily multiconfigurational. However, at both  $C_{2v}$  equilibrium geometries ( $^2A_1$  and  $^2B_2$ ), the orbitals are relatively well separated in energy. Therefore, at their equilibrium geometries, all the three lowest states are well described by the single-reference CCSD(T) method. Optimized geometries of the  $^2A_1$ ,  $^2B_2$ , and  $^4B_2$  states are shown in Fig. 5.

The 3,5-dehydrophenyl (1,3,5-tridehydrobenzene) anion ( $C_6H_3^-$ ) which was synthesized and studied<sup>25</sup> would be a precursor of  $C_6H_3$  in a photoelectron experiment.<sup>49</sup> As follows from the MO picture, the anion is a diradical. Indeed, in the lowest electronic states of  $C_6H_3^-$ , the  $10a_1$   $\sigma$  orbital is doubly occupied, while two other electrons are distributed in the  $11a_1$  and  $7b_2$   $\sigma$  orbitals. Hund's rule predicts the ground state of the anion to be a triplet. However, the reactivity of the anion gives indirect evidence that its ground state is a singlet state, although the triplet ground state could not be ruled out.<sup>25</sup> As in the case of the quartet state in  $C_6H_3$ , the triplet  $^3B_2$  ( $^3A_2'$ ) state of  $C_6H_3^-$  prefers  $D_{3h}$  geometry. We found that, in accordance with Hund's rule, at this geometry the singlet states are higher in energy (see Fig. 4).<sup>50</sup> The degeneracy between the closed- and open-shell singlets result in the Jahn–Teller distortions that lift the symmetry of both singlets. While the open-shell singlet  $^1B_2$  is, most likely, a transition state, the closed-shell  $^1A_1$  singlet is a real minimum. Its structure of  $C_{2v}$  symmetry is similar to the structure of the  $1^2A_1$  doublet state of the neutral. The equi-

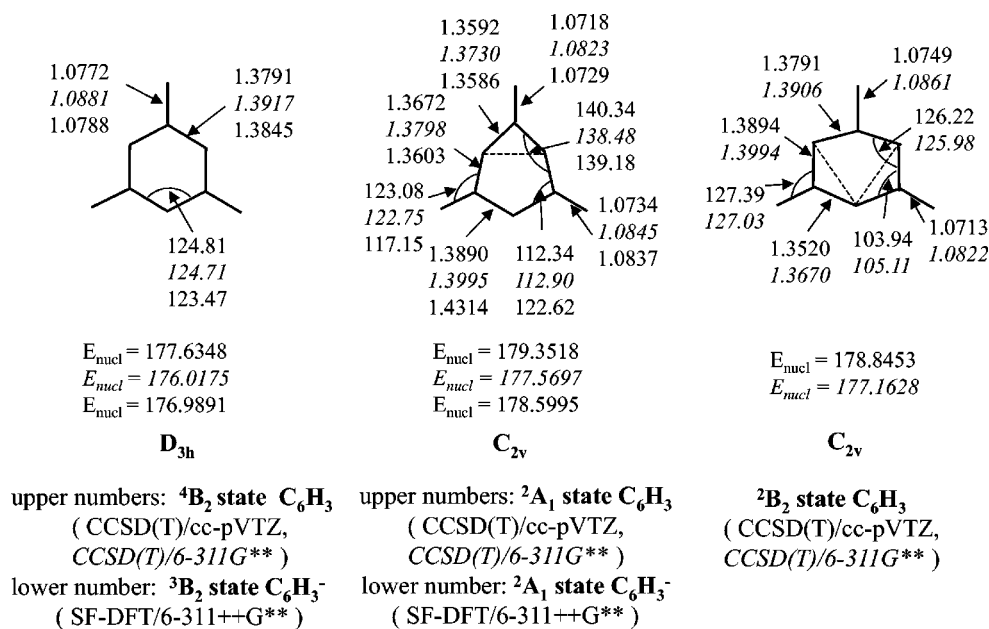


FIG. 5. Optimized geometries of the  $^4B_2$ ,  $^2A_1$ , and  $^2B_2$  states of  $C_6H_3$  [at the CCSD(T)/cc-pVTZ and CCSD(T)/6-311G\*\* levels] and of the  $^3B_2$  and  $^1A_1$  state of  $C_6H_3^-$  (at the SF-DFT/6-311++G\*\* level). Bond lengths are in angstroms, angles in degrees, and nuclear repulsion energies in hartrees.

TABLE I. Vertical excitation energies (eV) of 1,3,5-tridehydrobenzene calculated at the equilibrium geometries of the  ${}^3B_2$  and  ${}^1A_1$  states of the 3,5-dehydrophenyl anion.<sup>a</sup>

| State        | Type <sup>b</sup>                                  | From the ${}^3B_2$ geometry <sup>c</sup> | From the ${}^1A_1$ geometry <sup>c</sup> |
|--------------|--|--|--|
| $1\ {}^2A_1$ | $\sigma \rightarrow \sigma$ (allowed, allowed)     | -229.77026                               | -229.76228 <sup>d</sup>                  |
| $1\ {}^2B_2$ | $\sigma \rightarrow \sigma$ (allowed, forbidden)   | 0.000                                    | 1.987                                    |
| $1\ {}^4B_2$ | $\sigma \rightarrow \sigma$ (allowed, forbidden)   | 0.808                                    | 2.358                                    |
| $1\ {}^4B_1$ | $\pi \rightarrow \sigma$ (allowed, forbidden)      | 2.324                                    | 3.560                                    |
| $1\ {}^4A_2$ | $\pi \rightarrow \sigma$ (allowed, forbidden)      | 2.324                                    | 3.733                                    |
| $2\ {}^4A_2$ | $\pi \rightarrow \sigma$ (allowed, forbidden)      | 3.922                                    | 7.492                                    |
| $2\ {}^2A_1$ | $\sigma \rightarrow \sigma$ (forbidden, allowed)   | 4.267                                    | 3.098                                    |
| $2\ {}^2B_2$ | $\sigma \rightarrow \sigma$ (forbidden, forbidden) | 4.267                                    | 5.983                                    |
| $1\ {}^6B_2$ | $\pi \rightarrow \pi$ (forbidden, forbidden)       | 4.386                                    | 5.853                                    |
| $1\ {}^6A_1$ | $\pi \rightarrow \pi$ (forbidden, forbidden)       | 5.313                                    | 6.311                                    |
| $2\ {}^6B_2$ | $\pi \rightarrow \pi$ (forbidden, forbidden)       | 5.313                                    | 6.989                                    |
| $3\ {}^2A_1$ | $\sigma \rightarrow \sigma$ (forbidden, forbidden) | 5.291                                    | 8.066                                    |
| $3\ {}^2B_2$ | $\sigma \rightarrow \sigma$ (allowed, forbidden)   | 6.069                                    | 7.232                                    |
| $2\ {}^6A_1$ | $\pi \rightarrow \pi$ (forbidden, forbidden)       | 6.467                                    | 8.420                                    |

<sup>a</sup>Vertical excitation energies are calculated by the SF-CCSD method in the mixed (cc-pVTZ on carbon and cc-pVDZ on hydrogen) basis set.

<sup>b</sup>In parentheses, it is shown whether a state is accessible through a one-electron transition from the triplet and the singlet states of the anion, respectively.

<sup>c</sup>The equilibrium geometries of the anion are used (see Fig. 5).

<sup>d</sup>This energy is 0.217 eV higher than the  $1\ {}^2A_1$  state energy at the triplet anion geometry.

librium geometries of the  ${}^3B_2$  and  ${}^1A_1$  anion's states are shown in Fig. 5. Our preliminary calculations<sup>50</sup> show that *adiabatically* the  ${}^3B_2$  and  ${}^1A_1$  states are very close in energy.<sup>51</sup> The detailed study of the  $C_6H_3^-$  will be reported elsewhere.

### A. Vertical and adiabatic excitation energies

Since determining vertical energy separations from photoelectron spectra is straightforward, the availability of calculated vertical excitation energies at the anion geometry is useful in the experimental design and interpretation. We present the vertical excitation energies from both singlet  ${}^1A_1$  and triplet  ${}^3B_2$  anion's equilibrium geometries (Table I), because the adiabatic energy gap between the singlet and triplet states of the anion is very small. At the  $D_{3h}$  geometry of the  ${}^3B_2$  ( ${}^3A_2'$ ) state of  $C_6H_3^-$ , there are three pairs of degenerate orbitals: two pairs of  $\pi$  orbitals ( $1a_2/2b_1$  and  $2a_2/3b_1$ ) and the  $11a_1/7b_2$  orbitals. Therefore, the  $1\ {}^2A_1$  and  $1\ {}^2B_2$  doublets ( ${}^2E'$  at  $D_{3h}$ ) are degenerate. These two doublets correspond to configurations (e) and (g) in Fig. 2. At the SF-CCSD level in a mixed cc-pVTZ/cc-pVDZ basis (see Sec. II C), the quartet  $1\ {}^4B_2$  state is 0.8 eV higher in energy than the doublets. We used a high-spin component of this quartet as the SF reference.

The next two degenerate states, the  $1\ {}^4A_2$  and  $1\ {}^4B_1$  quartets, are derived from the excitation of an electron from the  $2b_1$  or  $1a_2$   $\pi$  orbital to the  $10a_1$  orbital (see Fig. 3). These degenerate states can also undergo Jahn-Teller distortions. These quartets lie approximately 2.3 eV above the doublets. The relatively low excitation energies of these states indicate a strong interaction between the  $\pi$  and  $\sigma$  systems in 1,3,5-tridehydrobenzene. These quartets, as well as other states that include electron excitations between the  $\pi$  and  $\sigma$  orbitals, do not belong to the triradical states, i.e., states derived by distributing three electrons between three energetically close orbitals ( $10a_1$ ,  $11a_1$ , and  $7b_2$ ). As explained in

Sec. II A, triradical states are well described by the SF approach. However, states derived by excitations out of the subspace of the three triradical orbitals are treated by the SF methods in a less balanced way. For example, the wave function for the  $1\ {}^4A_2$  quartet consists of three determinants [similar to state (b) from Fig. 2]:

$$\Psi_{4A_2} \sim 2b_1 11a_1 7b_2 |\alpha\alpha\beta\rangle + 2b_1 11a_1 7b_2 |\beta\alpha\alpha\rangle + 2b_1 11a_1 7b_2 |\beta\alpha\alpha\rangle. \quad (3)$$

One of these determinants,  $2b_1 11a_1 7b_2 |\beta\alpha\alpha\rangle$ , is a single spin-flip excitation from the  $10a_1 11a_1 7b_2 |\alpha\alpha\alpha\rangle$  reference. However, two other determinants are doubly excited configurations with respect to the reference. Therefore, the SF description of this state is not well balanced, which is reflected in the spin contamination of the wave function.<sup>52</sup> To understand how accurately these states are described by SF, we performed additional calculations (at a slightly different  $D_{3h}$  geometry). Table II compares the SF-CCSD vertical excitation energies against those calculated by the MCSCF and MCQPPT2 methods.<sup>53</sup> As seen from Table II, the SF-CCSD results are in excellent agreement with the MCQPPT2 ones both for the  $1\ {}^2A_1/1\ {}^2B_2-1\ {}^4B_2$  transition (all these are the triradical states which are well described by SF) and for the  $1\ {}^2A_1/1\ {}^2B_2-1\ {}^4B_1/1\ {}^4A_2$  transition (the  $1\ {}^4B_1/1\ {}^4A_2$  states are spin contaminated at the SF-CCSD level).

TABLE II. Vertical excitation energies (eV).<sup>a</sup>

| Method/basis     | $1\ {}^2A_1/1\ {}^2B_2$ | $1\ {}^4B_2$ | $1\ {}^4B_1/1\ {}^4A_2$ |
|------------------|-------------------------|--------------|-------------------------|
| MCSCF/6-311G**   | -228.851857             | 0.726        | 2.281                   |
| MCQPPT2/6-311G** | -229.575314             | 0.719        | 2.055                   |
| SF-CCSD/6-311G** | -229.679943             | 0.726        | 2.155                   |

<sup>a</sup>Calculated at the  $D_{3h}$  geometry.

The next state in Table I,  $2^4A_2$ , also involves  $\pi$ - $\sigma$  excitations. In the dominant configuration of this state, the  $1b_1$ ,  $11a_1$ , and  $7b_2$  orbitals are singly occupied, while the  $2b_1$ ,  $1a_2$ , and  $10a_1$  orbitals are doubly occupied. However, two configurations with orbitals  $2b_1$ ,  $10a_1$ , and  $7b_2$  or  $1a_2$ ,  $10a_1$ , and  $11a_1$ , being singly occupied, have large coefficients. The next two states are a degenerate pair of the  $2^2A_1$  and  $2^2B_2$  doublets [(i) and (d) states from Fig. 2]. These states are similar to the closed- and open-shell singlets in diradical systems. They are degenerate at  $D_{3h}$  geometries because of the exact degeneracy between the  $11a_1$  and  $7b_2$  orbitals [similar to the  $1^1A_1$  and  $1^1B_2$  states of TMM (Ref. 34)]. Four sextet states  $1^6A_1$ ,  $2^6A_1$ ,  $1^6B_2$ , and  $2^6B_2$ , two of them exactly degenerate, are derived from excitations from the  $2b_1$  or  $1a_2$  to the  $3b_1$  or  $2a_2$   $\pi$  orbitals. In this energy region, there are several other states derived from excitations between  $\sigma$  and  $\pi$  systems (not shown in Table I). The counterpart of the  $2^2A_1$  state (i) is the closed-shell doublet  $3^2A_1$  (j) at 5.3 eV. The open-shell doublet  $3^2B_2$  of type (c) lies at approximately 6.1 eV.

At the equilibrium geometry of the  $^1A_1$  anion's state the energy of the  $1^2A_1$  state of  $C_6H_3$  is approximately 0.2 eV higher than its energy at the triplet anion's geometry. The strongly distorted geometry of the anion's singlet state leads to large energy splittings between the states that are degenerate at  $D_{3h}$  symmetry. Thus, the  $1^2B_2$  doublet state (which is degenerate with the  $1^2A_1$  doublet at  $D_{3h}$  geometry) lies about 2 eV higher in energy. The  $1^4B_2$  quartet state is 2.4 eV higher in energy. Relative to the  $D_{3h}$  geometry, the excitation energy of the closed-shell doublet of type (i) in Fig. 2,  $2^2A_1$ , becomes lower, while the energy of its counterpart, the  $2^2B_2$  doublet of type (d), rises.

The adiabatic energy separations between the ground  $^2A_1$  and the excited  $^2B_2$  and  $^4B_2$  states are presented in Table III. All adiabatic energies are calculated at the CCSD(T)/cc-pVTZ equilibrium geometries, except for the CCSD/6-311G\*\* and CCSD(T)/6-311G\*\* values which are calculated at the CCSD(T)/6-311G\*\* geometries. The zero-point energies (ZPEs) are calculated at the CCSD(T)/6-311G\*\* level. At the highest level of theory, CCSD(T)/cc-pVTZ, the energy gap between the  $^2A_1$  and  $^2B_2$  doublets is 0.223 eV (5.14 kcal/mol) and the splitting between the  $^2A_1$  doublet and the  $^4B_2$  quartet is 1.375 eV (31.71 kcal/mol). The SF-CCSD energy separations in the mixed basis set are 0.082 eV (1.89 kcal/mol) and 1.200 eV (27.67 kcal/mol) for the  $^2A_1$ - $^2B_2$  and  $^2A_1$ - $^4B_2$  transitions, respectively. Applying Eq. (2), we have obtained similar results for the SF-CCSD/cc-pVTZ splittings: 0.082 eV and 1.193 eV. The SF-CIS(D) results are very close to the SF-CCSD ones: the discrepancy is less than 2 kcal/mol. The SF-CCSD values differ from the CCSD(T) ones by no more than 4 kcal/mol. The SF-CCSD energy separations between states are much closer to the CCSD(T) ones than the CCSD results are. We have observed the similar behavior of the SF methods in the methylene example (Sec. III B in Ref. 34).

TABLE III. Total energies (hartree) for the ground  $^2A_1$  state and adiabatic excitation energies (eV) for the low-lying excited states.<sup>a</sup>

| Method/basis                  | $^2A_1$     | $^2B_2$ | $^4B_2$ |
|-------------------------------|-------------|---------|---------|
| CCSD/6-311G** <sup>b</sup>    | -229.691737 | -0.039  | 0.757   |
| CCSD(T)/6-311G** <sup>b</sup> | -229.748061 | 0.203   | 1.256   |
| SF-CIS(D)/6-311G**            | -229.602587 | 0.104   | 1.010   |
| SF-CCSD/6-311G**              | -229.695974 | 0.065   | 1.086   |
| SF-CIS(D)/mixed <sup>c</sup>  | -229.699820 | 0.122   | 1.124   |
| SF-CCSD/mixed <sup>c</sup>    | -229.793207 | 0.082   | 1.200   |
| CCSD/cc-pVTZ                  | -229.798697 | 0.018   | 0.885   |
| CCSD(T)/cc-pVTZ               | -229.864320 | 0.223   | 1.375   |
| SF-CIS(D)/cc-pVTZ             | -229.718160 | 0.122   | 1.117   |
| SF-CCSD/cc-pVTZ <sup>d</sup>  | -229.793207 | 0.082   | 1.193   |
| SF-CCSD/cc-pVTZ <sup>e</sup>  | -229.811547 | 0.082   | 1.193   |
| $\Delta ZPE^f$                |             | -0.021  | 0.010   |

<sup>a</sup>All values are calculated at the CCSD(T)/cc-pVTZ optimized geometries (see Fig. 5), except when specified otherwise.

<sup>b</sup>Calculated at the CCSD(T)/6-311G\*\* optimized geometries.

<sup>c</sup>Mixed basis set: cc-pVTZ on carbon and cc-pVDZ on hydrogen.

<sup>d</sup>Determined by using Eq. (2) from the 6-311G\*\* and cc-pVTZ bases.

<sup>e</sup>Determined by using Eq. (2) from the mixed (cc-pVTZ on carbon and cc-pVDZ on hydrogen) and cc-pVTZ bases.

<sup>f</sup>Calculated at the CCSD(T)/6-311G\*\* level.

## B. Structures and vibrational frequencies of the $1^2A_1$ , $1^2B_2$ , and $1^4B_2$ states of $C_6H_3$

In the context of photoelectron spectroscopy, analyses of equilibrium properties of anion and neutral states are extremely important. This section discusses the structures and vibrational frequencies of the lowest electronic states of  $C_6H_3$ , while a detailed analysis of anion's properties will be reported elsewhere.

Figure 6 compares the structures of the lowest 1,3,5-tridehydrobenzene states with the structures of two m-benzyne's states<sup>34</sup> and the benzene ground state.<sup>54</sup> As structural characteristics, we choose the  $C_1$ - $C_3$  and  $C_1$ - $C_5$  diagonal lengths (carbons 1, 3, and 5 are radical centers in 1,3,5-tridehydrobenzene, carbons 1 and 3 are radical centers in m-benzyne), as well as the  $C_2$ - $C_4$  and  $C_2$ - $C_6$  diagonal lengths (these carbons are connected to hydrogens in all the molecules). These distances are shown in Fig. 6. In benzene, all the C-C diagonals are equal. In both the quartet state of 1,3,5-tridehydrobenzene and the triplet state of m-benzyne the diagonal lengths are contracted relative to benzene. This indicates that there is some bonding between the same-spin radical centers. This is because removing a hydrogen results in an increase in electronic density in the central part of the molecule. This additional electronic density bonds the radical centers even in the high-spin states. Overall, the structures of the high-spin states of  $m$ - $C_6H_4$  and  $C_6H_3$  are very similar. Likewise, there is also a similarity between the  $^1A_1$  state of m-benzyne and the  $1^2A_1$  state of  $C_6H_3$ . However, the  $C_1$ - $C_3$  diagonal in 1,3,5-tridehydrobenzene is slightly shorter than the corresponding length in m-benzyne, due to the interaction of the unpaired electron on the  $C_3$  carbon of 1,3,5-tridehydrobenzene with the electron density on the  $C_1$  and  $C_5$  carbons.<sup>55</sup> As expected, the structure of the  $1^2B_2$  transition state has a long  $C_1$ - $C_5$  diagonal and two short  $C_1$ - $C_3$  and  $C_3$ - $C_5$  diagonals. The structure is less tight than the structure of the ground  $1^2A_1$  state. Most of the diagonal

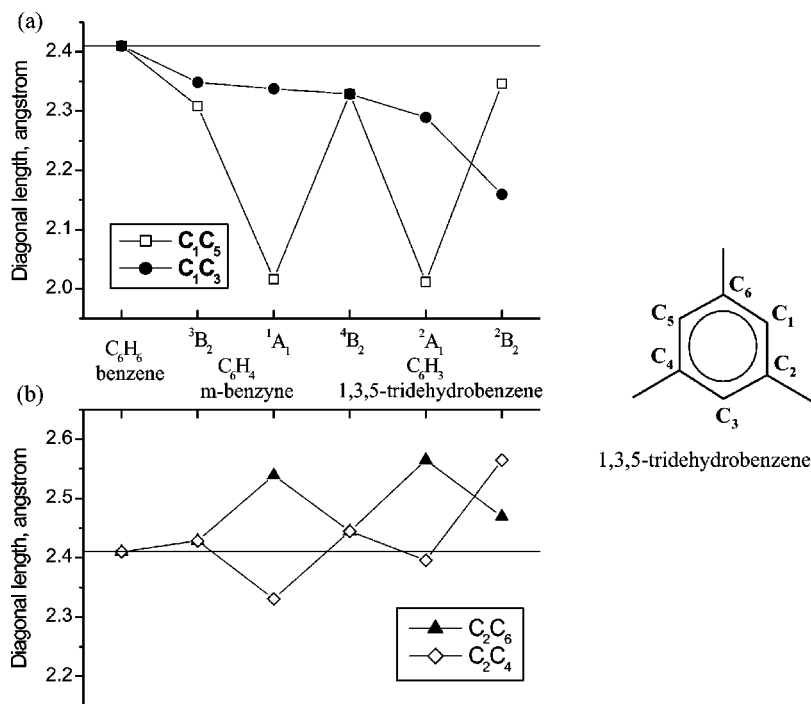


FIG. 6. Diagonal distances in the  ${}^4B_2$ ,  ${}^2A_1$ , and  ${}^2B_2$  states of 1,3,5-tridehydrobenzene and in the  ${}^3B_2$  and  ${}^1A_1$  states of m-benzynes as compared with the corresponding distances in benzene. Upper panel (a) shows distances between the radical centers. Lower panel (b) presents distances between nonradical carbons (i.e., those which are connected to hydrogens in all molecules).

lengths between the nonradical carbons in 1,3,5-tridehydrobenzene and m-benzynes are longer than the ones in benzene. However, this increase is smaller than the contraction of the distances between the dehydrocarbons; i.e., the overall rigidity of the molecular structures increases relative to benzene.

Table IV presents the vibrational frequencies of the three lowest electronic states of  $C_6H_3$ . The frequencies of the skeleton modes are compared with the corresponding benzene's vibrations. As mentioned above, the  $1^2B_2$  state is a

transition state with one imaginary frequency  $\omega_5$ . This mode connects the structure with one of the real minima. The real minimum on the potential surface, the  $1^2A_1$  state, is also less stable to ring deformations, which correspond to the pseudorotations (modes  $\omega_4$ – $\omega_5$ ) relative to the undistorted quartet  $1^4B_2$  state of  $C_6H_3$  and benzene. Due to  $\pi$ -system destabilization, lowering of the high-order symmetry of benzene makes the  $C_6H_3$  structures less stable with respect to other ring deformations (e.g., modes  $\omega_9$  and  $\omega_{11}$ – $\omega_{12}$ ). Moreover, the out-of-plane (OPLA) ring deformation frequencies

TABLE IV. Vibrational frequencies of the  $1^2A_1$ ,  $1^2B_2$ , and  $1^4B_2$  states of 1,3,5-tridehydrobenzene ( $\text{cm}^{-1}$ ).<sup>a</sup>

|               | Symm. <sup>b</sup> | Type of mode       | Benzene <sup>c</sup>   | $1^4B_2$ | $1^2A_1$ | $1^2B_2$ |
|---------------|--------------------|--------------------|------------------------|----------|----------|----------|
| $\omega_1$    | $a_2 (e'')$        | Ring deform (OPLA) | 410 ( $\omega_{20}$ )  | 322      | 506      | 439      |
| $\omega_2$    | $b_1 (e'')$        | Ring deform (OPLA) | 410 ( $\omega_{20}$ )  | 322      | 415      | 470      |
| $\omega_3$    | $b_1 (a_2'')$      | Ring deform (OPLA) | 703 ( $\omega_8$ )     | 576      | 482      | 482      |
| $\omega_4$    | $a_1 (e')$         | Ring deform        | 606 ( $\omega_{18}$ )  | 607      | 382      | 505      |
| $\omega_5$    | $b_2 (e')$         | Ring deform        | 606 ( $\omega_{18}$ )  | 607      | 444      | 160i     |
| $\omega_6$    | $b_1 (a_2'')$      | CH bend (OPLA)     |                        | 749      | 742      | 739      |
| $\omega_7$    | $a_2 (e'')$        | CH bend (OPLA)     |                        | 791      | 801      | 778      |
| $\omega_8$    | $b_1 (e'')$        | CH bend (OPLA)     |                        | 791      | 803      | 827      |
| $\omega_9$    | $a_1 (a_1')$       | Ring deform        | 1010 ( $\omega_6$ )    | 965      | 798      | 799      |
| $\omega_{10}$ | $a_1 (a_1')$       | Ring str           | 992 ( $\omega_2$ )     | 1028     | 1085     | 1081     |
| $\omega_{11}$ | $a_1 (e')$         | Ring str+deform    | 1486 ( $\omega_{13}$ ) | 1054     | 1068     | 1011     |
| $\omega_{12}$ | $b_2 (e')$         | Ring str+deform    | 1486 ( $\omega_{13}$ ) | 1054     | 991      | 1056     |
| $\omega_{13}$ | $b_2 (a_2')$       | Ring str           | 1310 ( $\omega_9$ )    | 1195     | 1225     | 1212     |
| $\omega_{14}$ | $b_2 (a_2')$       | CH bend            |                        | 1230     | 1208     | 1232     |
| $\omega_{15}$ | $a_1 (e')$         | CH bend            |                        | 1361     | 1350     | 1281     |
| $\omega_{16}$ | $b_2 (e')$         | CH bend            |                        | 1361     | 1323     | 1379     |
| $\omega_{17}$ | $a_1 (e')$         | Ring str           | 1596 ( $\omega_{16}$ ) | 1569     | 1710     | 1510     |
| $\omega_{18}$ | $b_2 (e')$         | Ring str           | 1596 ( $\omega_{16}$ ) | 1569     | 1516     | 1695     |
| $\omega_{19}$ | $a_1 (e')$         | CH str             |                        | 3189     | 3231     | 3253     |
| $\omega_{20}$ | $b_2 (e')$         | CH str             |                        | 3189     | 3230     | 3252     |
| $\omega_{21}$ | $a_1 (a_1')$       | CH str             |                        | 3191     | 3248     | 3216     |

<sup>a</sup>All  $C_6H_3$  frequencies are calculated at the CCSD(T)/6-311++G\*\* level at the CCSD(T)/6-311++G\*\* optimized geometries (see Fig. 5).

<sup>b</sup>Symmetry labels are given in  $C_{2v}$  and  $D_{3h}$  (in parentheses) symmetry groups.

<sup>c</sup>Reference 56; a description of the benzene's modes is given in Ref. 57.

( $\omega_1 - \omega_3$ ) of all the three states of  $C_6H_3$  are lower than in benzene. The decrease is due to the weaker conjugation of the  $\pi$  system in the distorted (relative to benzene) structures of  $C_6H_3$ . Some ring stretching frequencies, however, do not significantly change or even become higher in  $C_6H_3$  (e.g., the symmetric breathing mode  $\omega_{10}$  and  $\omega_{17} - \omega_{18}$  modes). The behavior of these modes is consistent with the structural changes in the different  $C_6H_3$  states discussed above.

#### IV. CONCLUSIONS

Triradicals are difficult to describe by electronic structure methods due to orbital degeneracies. However, the spin-flip approach can be extended to these systems. The electronic structure of the 1,3,5-tridehydrobenzene triradical has been characterized by the SF and CCSD(T) methods. We find that the ground state of the molecule is the Jahn–Teller distorted doublet  ${}^2A_1$  which has a  $C_{2v}$  structure similar to the geometry of m-benzyne. The second doublet state  ${}^2B_2$ , which lies only 0.1–0.2 eV higher in energy, is a transition state with one imaginary frequency. The  $4A_2'$  quartet state has  $D_{3h}$  symmetry and is 1.2–1.4 eV higher in energy. The analysis of the equilibrium properties of these states should be useful in planning and interpreting photoelectron experiments.

#### ACKNOWLEDGMENTS

Support from the National Science Foundation CAREER Award (Grant No. CHE-0094116), the Camille and Henry Dreyfus New Faculty Awards Program, and the Donors of the Petroleum Research Fund administered by the American Chemical Society (PRF-AC grant), and the WISE Research Fund (USC) is gratefully acknowledged. We would like to thank Professor W. C. Lineberger for introducing us to the exciting subject of triradicals and Professor P. G. Wenthold for stimulating discussions.

- <sup>1</sup>L. Salem and C. Rowland, *Angew. Chem. Int. Ed. Engl.* **11**, 92 (1972).
- <sup>2</sup>T. Saito, A. Ito, and K. Tanaka, *J. Phys. Chem.* **102**, 8021 (1998).
- <sup>3</sup>E. C. Brown and W. T. Borden, *J. Phys. Chem.* **106**, 2963 (2002).
- <sup>4</sup>C. R. Kemnitz, R. R. Squires, and W. T. Borden, *J. Am. Chem. Soc.* **119**, 6564 (1997).
- <sup>5</sup>L. A. Hammad and P. G. Wenthold, *J. Am. Chem. Soc.* **123**, 12311 (2001).
- <sup>6</sup>A. Rajca, *Chem. Rev.* **94**, 871 (1994).
- <sup>7</sup>B. L. V. Prasad and T. P. Radhakrishnan, *J. Phys. Chem.* **101**, 2973 (1997).
- <sup>8</sup>T. D. Selby, K. R. Stickley, and S. C. Blackstock, *Org. Lett.* **2**, 171 (2000).
- <sup>9</sup>K. Sato, M. Yano, M. Furuichi *et al.*, *J. Am. Chem. Soc.* **119**, 6607 (1997).
- <sup>10</sup>T. Weyland, K. Costuas, A. Mari, J. Halet, and C. Lapinte, *Organometallics* **17**, 5569 (1998).
- <sup>11</sup>Y. Hosokoshi, K. Katoh, Y. Nakazawa, H. Nakano, and K. Inoue, *J. Am. Chem. Soc.* **123**, 7921 (2001).
- <sup>12</sup>S. G. Wierschke, J. J. Nash, and R. R. Squires, *J. Am. Chem. Soc.* **115**, 11958 (1993).
- <sup>13</sup>R. R. Squires and C. J. Cramer, *J. Phys. Chem.* **102**, 9072 (1998).
- <sup>14</sup>C. J. Cramer, J. J. Nash, and R. R. Squires, *Chem. Phys. Lett.* **277**, 311 (1997).
- <sup>15</sup>H. F. Bettinger, P. v. R. Schleyer, and H. F. Schaefer III, *J. Am. Chem. Soc.* **121**, 2829 (1999).
- <sup>16</sup>W. Sander, *Acc. Chem. Res.* **32**, 669 (1999).
- <sup>17</sup>T. D. Crawford, E. Kraka, J. F. Stanton, and D. Cremer, *J. Chem. Phys.* **114**, 10638 (2001).
- <sup>18</sup>P. G. Wenthold, R. R. Squires, and W. C. Lineberger, *J. Am. Chem. Soc.* **120**, 5279 (1998).

- <sup>19</sup>J. G. Radziszewski, M. R. Nimlos, P. R. Winter, and G. B. Ellison, *J. Am. Chem. Soc.* **118**, 7400 (1996).
- <sup>20</sup>H. F. Bettinger, P. v. R. Schleyer, and H. F. Schaefer III, *J. Am. Chem. Soc.* **121**, 2829 (1999).
- <sup>21</sup>H. A. Lardin, J. J. Nash, and P. G. Wenthold, *J. Am. Chem. Soc.* **124**, 12 612 (2002).
- <sup>22</sup>J. Chandrasekhar, E. D. Jemmis, and P. v. R. Schleyer, *Tetrahedron Lett.* **39**, 3707 (1979).
- <sup>23</sup>P. v. R. Schleyer, H. Jiao, M. N. Glukhovtsev, J. Chandrasekhar, and E. Kraka, *J. Am. Chem. Soc.* **116**, 10129 (1994).
- <sup>24</sup>E. D. Nelson and H. I. Kenttamaa, *J. Am. Soc. Mass Spectrom.* **12**, 258 (2001).
- <sup>25</sup>J. Hu and R. R. Squires, *J. Am. Chem. Soc.* **118**, 5816 (1996).
- <sup>26</sup>A. I. Krylov, *Chem. Phys. Lett.* **338**, 375 (2001).
- <sup>27</sup>A. I. Krylov and C. D. Sherrill, *J. Chem. Phys.* **116**, 3194 (2002).
- <sup>28</sup>A. I. Krylov, *Chem. Phys. Lett.* **350**, 522 (2001).
- <sup>29</sup>Y. Shao, M. Head-Gordon, and A. I. Krylov, *J. Chem. Phys.* **118**, 4807 (2003).
- <sup>30</sup>J. S. Sears, C. D. Sherrill, and A. I. Krylov *J. Chem. Phys.* (to be published).
- <sup>31</sup>G. D. Purvis and R. J. Bartlett, *J. Chem. Phys.* **76**, 1910 (1982).
- <sup>32</sup>G. E. Scuseria and H. F. Schaefer, *Chem. Phys. Lett.* **142**, 354 (1987).
- <sup>33</sup>C. D. Sherrill, A. I. Krylov, E. F. C. Byrd, and M. Head-Gordon, *J. Chem. Phys.* **109**, 4171 (1998).
- <sup>34</sup>L. V. Slipchenko and A. I. Krylov, *J. Chem. Phys.* **117**, 4694 (2002).
- <sup>35</sup>P. Piecuch, S. A. Kucharski, and R. J. Bartlett, *J. Chem. Phys.* **110**, 6103 (1999).
- <sup>36</sup>B. O. Roos, P. R. Taylor, and P. E. M. Siegbahn, *Chem. Phys.* **48**, 157 (1980).
- <sup>37</sup>K. Ruedenberg, M. W. Schmidt, M. M. Gilbert, and S. T. Elbert, *Chem. Phys.* **71**, 41 (1982).
- <sup>38</sup>H. Nakano, *J. Chem. Phys.* **99**, 7983 (1993).
- <sup>39</sup>R. Krishnan, J. S. Binkley, R. Seeger, and J. A. Pople, *J. Chem. Phys.* **72**, 650 (1980).
- <sup>40</sup>T. H. Dunning, *J. Chem. Phys.* **90**, 1007 (1989).
- <sup>41</sup>T. Clark, J. Chandrasekhar, and P. v. R. Schleyer, *J. Comput. Chem.* **4**, 294 (1983).
- <sup>42</sup>Basis sets were obtained from the Extensible Computational Chemistry Environment Basis Set Database, Version, as developed and distributed by the Molecular Science Computing Facility, Environmental and Molecular Sciences Laboratory which is part of the Pacific Northwest Laboratory, P.O. Box 999, Richland, WA 99352, and funded by the U.S. Department of Energy. The Pacific Northwest Laboratory is a multiprogram laboratory operated by Battelle Memorial Institute for the U.S. Department of Energy under Contract No. DE-AC06-76RLO 1830. Contact David Feller or Karen Schuchardt for further information.
- <sup>43</sup>J. Kong, C. A. White, A. I. Krylov *et al.*, *J. Comput. Chem.* **21**, 1532 (2000).
- <sup>44</sup>J. F. Stanton, J. Gauss, J. D. Watts, W. J. Lauderdale, and R. J. Bartlett, computer code ACES II, 1993. The package also contains modified versions of the MOLECULE Gaussian integral program of J. Almlöf and P. R. Taylor, the ABACUS integral derivative program written by T. U. Helgaker, H. J. Aa. Jensen, P. Jørgensen, and P. R. Taylor, and the PROPS property evaluation integral code of P. R. Taylor.
- <sup>45</sup>M. W. Schmidt, K. K. Baldrige, J. A. Boatz *et al.*, *J. Comput. Chem.* **14**, 1347 (1993).
- <sup>46</sup>H. A. Jahn and E. Teller, *Proc. R. Soc. London, Ser. A* **161**, 220 (1937).
- <sup>47</sup>In a system with a threefold axis the potential surface of the Jahn–Teller distortions consists of three equivalent minima and three transition states connecting them [E. R. Davidson and W. T. Borden, *J. Phys. Chem.* **87**, 4783 (1983)]. Pseudorotation between each pair of the equivalent minima proceeds through one of the equivalent transition states and vice versa.
- <sup>48</sup>This is different from, for example, trimethylenemethane, where the open-shell singlet  ${}^1B_2$  undergoes a second-order Jahn–Teller distortion by rotating one of the methylene groups and disrupting the conjugated  $\pi$ -system of the molecule.
- <sup>49</sup>P. G. Wenthold and W. C. Lineberger (private communication).
- <sup>50</sup>L. V. Slipchenko, M. Nooijen, and A. I. Krylov (preliminary results).
- <sup>51</sup>The singlet–triplet adiabatic energy separation is less than 1 kcal/mol on the SF-DFT/6-311++G\*\* level, the singlet state being lower in energy.
- <sup>52</sup>This is similar to some excited states in radicals [D. Maurice and M. Head-Gordon, *J. Phys. Chem.* **100**, 6131 (1996)]. Despite this, the EOM–CCSD method treats such states accurately.
- <sup>53</sup>The active space includes all orbitals and electrons shown in Fig. 3, i.e.,



six  $\pi$  orbitals and three  $\sigma$  orbitals, and nine electrons ( $9 \times 9$ ). Root averaging was used to calculate the degenerate states.

<sup>54</sup>J. Gauss and J. F. Stanton, *J. Phys. Chem. A* **104**, 2865 (2000).

<sup>55</sup>This interaction is stronger than, for example, the interaction of a radical center with nonradical carbons in phenyl: the corresponding length in phenyl is 2.370 Å (Ref. 19) which is about 0.09 Å longer than the length in the  $^2A_1$  state of 1,3,5-tridehydrobenzene.

<sup>56</sup>T. Shimanouchi, *Tables of Molecular Vibrational Frequencies Consolidated*, National Bureau of Standards (U.S. GPO, Washington, D.C., 1972), Vol. I.

<sup>57</sup>G. Herzberg, *Molecular Spectra and Molecular Structure: Infrared and Raman Spectra of Polyatomic Molecules* (van Nostrand Reinhold, New York, 1945), Vol. III.